INCREMENTAL IDENTIFICATION OF TRANSPORT COEFFICIENTS IN CONVECTION-DIFFUSION SYSTEMS

MAKA KARALASHVILI*, SVEN GROß†, ADEL MHAMDI*, ARNOLD REUSKEN†, AND WOLFGANG MARQUARDT*

Abstract. In this paper, an incremental approach for the identification of a model for transport coefficients in convection-diffusion systems on the basis of high-resolution measurement data is presented. The transport is represented by a convection term with known convective velocity and by a diffusion term with an unknown, generally state-dependent transport coefficient. The identification of the transport model for this transport coefficient constitutes an ill-posed nonlinear inverse problem. We present a novel decomposition approach in which this inverse problem is split into a sequence of inverse subproblems. In the first identification step of this incremental approach a source is estimated by solving an affine-linear inverse problem by means of the conjugate gradient method. In the second identification step a nonlinear inverse problem has to be solved in order to reconstruct a transport coefficient. A Newton-type method using the conjugate gradient method in its inner iteration is used to solve this nonlinear inverse problem of coefficient estimation. Finally, in the third identification step a transport model structure is proposed and identified on the basis of the model-free transport coefficient reconstructed in the two previous steps. The ill-posedness of each inverse problem is examined by using artificially perturbed transient simulation data and appropriate regularization techniques. The identification methodology is illustrated for a three-dimensional convection-diffusion equation which has its origin in the modeling and simulation of energy transport in a laminar wavy film flow.

Key words. Modeling, transport phenomena, convection-diffusion equation, inverse problem, regularization, conjugate gradient method, inexact Newton-type method, parameter estimation, identification.

AMS subject classifications. 15A15, 15A09, 15A23

1. Introduction.

Let $\Omega \subset \mathbb{R}^3$ be a computational domain, with boundary parts $\partial\Omega = \Gamma_D \cup \Gamma_N$, where the indices D and N indicate the Dirichlet and Neumann parts of the boundary, respectively. We consider the convection-diffusion equation

$$\frac{\partial \rho u}{\partial t} + \nabla \cdot (\rho u \mathbf{w}) - \nabla \cdot (a \nabla u) = 0 \quad \text{in } \Omega \times (t_0, t_f]\,, \tag{1.1a}$$

with initial and boundary conditions

$$\begin{aligned} u(\mathbf{x}, t_0) &= u_0(\mathbf{x})\,, \quad \mathbf{x} \in \Omega\,, \\ u(\mathbf{x}, t) &= g_D(\mathbf{x}, t)\,, \quad (\mathbf{x}, t) \in \Gamma_D \times [t_0, t_f]\,, \\ \frac{\partial u}{\partial n}(\mathbf{x}, t) &= g_N(\mathbf{x}, t)\,, \quad (\mathbf{x}, t) \in \Gamma_N \times [t_0, t_f]\,. \end{aligned} \tag{1.1b}$$

The scalar state variable $u(\mathbf{x}, t)$ represents, e. g. specific enthalpy in case of energy transport or mass density in case of mass transport. $\rho(\mathbf{x}, t)$ stands for the density of the fluid. The vector field $\mathbf{w}(\mathbf{x}, t) \in \mathbb{R}^3$ represents velocity and is assumed to be known. The scalar function $a(\,\cdot\,)$ denotes the unknown, in general state-dependent, transport coefficient.

The transport coefficient describes complicated transport phenomena, for which a multitude of competing candidate model structures can be formulated on the basis

*AVT-Process Systems Engineering, RWTH Aachen University, Turmstrasse 46, D-52064 Aachen, Germany ({maka.karalashvili, adel.mhamdi, wolfgang.marquardt}@avt.rwth-aachen.de).

†Numerical Mathematics, RWTH Aachen University, Templergraben 55, D-52056 Aachen, Germany ({gross, reusken}@igpm.rwth-aachen.de).

of different assumptions and theories. Experimental data should be used to estimate parameters that occur in these candidate models and to discriminate between the competing candidate models using some reasonable measure of model validity.

The identification of transport coefficients from appropriate measurement data, such as temperature or concentration, belongs to the class of ill-posed inverse problems. Many studies on the estimation of transport coefficients are available. One possible solution technique is the so-called equation error method [12, 19, 28]. In that approach the transient measurement data are inserted in the model (1.1) which is then interpreted as a system of equations for the unknown coefficient. The integration of these equations results in a direct relationship between the measured data and the unknown coefficient values. This relationship is frequently quite complicated and the transport coefficient has to be determined using special problem-adapted methods. Thus, equation error methods are rather problem-dependent. Another well-established technique for the identification of transport coefficients, as a function of states and time, relies on an optimization-based formulation which is used in the framework of a *coefficient inverse problem*, cf. [2]. In this approach, the reconstruction of the transport coefficient in model (1.1) uses suitable transient measurement data $u_m(\mathbf{x},t)\,,(\mathbf{x},t)\in\Omega\times[t_0,t_f]$. It is often assumed that the initial and boundary conditions of the problem are known. Quite some literature is available on the subject (cf. [3, 11, 30] and the references therein); the treatment, however, is typically restricted to one or two space dimensions. Furthermore, these studies do not aim at the reconstruction of a suitable transport model (structure and parameters) for transport coefficients.

In the so-called *simultaneous* approach, problem (1.1) for the identification of a model (structure and parameters) for the transport coefficient is solved for each model candidate using, for example, one of the above mentioned techniques. This leads to a large number of complex estimation problems. As a consequence, the discrimination between competing transport model candidates requires high computational effort. Furthermore, if a model candidate for the transport coefficient contains uncertainty or structural errors, this approach often yields biased or poor estimates [31]. Often satisfactory results can only be achieved if the correct model structure for the transport coefficient is known. In the present work, in contrast, we use a fundamentally different, so-called *incremental* approach [23] for the identification of a structured model for the transport coefficient.

In the incremental identification approach, incremental *modeling* interplays with the incremental *identification*. In incremental modeling, the structure of a model to be identified is refined step by step by specifying submodels gradually in a sequence of successive refinement levels. Consequently, more transparency concerning the individual decisions during the modeling process can be gained. The incremental identification of a model reflects the steps of incremental modeling straightforwardly by splitting up the identification problem into a sequence of subproblems. The discrimination between the candidate models turns out to become more flexible as the replacement of a submodel on a certain model refinement level affects only the submodels on the following levels. Often this also leads to benefits in terms of less computational effort. The incremental strategy already proved to be an efficient and robust alternative for the mechanistic modeling of kinetic phenomena in multi-phase systems [24], the reconstruction of diffusion coefficients in liquids [6] and the identification of complex reaction kinetics in homogeneous systems [9].

In this paper, we present and investigate the incremental method of modeling and

identification for the class of inverse transport coefficient problems described by eq. (1.1). The application of the incremental approach to this class of problems is new. As a first step in the analysis of this technique we show, based on simulated data assuming a time- and space-dependent transport coefficient, that this coefficient can be reconstructed without using any *a-priori* knowledge on its functional representation. We assume, however, that the model structure for the parametric model of this transport coefficient is known. Nevertheless, the incremental identification technique can be directly applied for the case when the model structure is unknown and has to be determined from the data and prior knowledge on candidate model structures. Furthermore, in case of different model candidates for the transport coefficient, the additional procedure of model discrimination does not affect the overall technique described in this paper. We analyse this identification approach and show that the method yields satisfactory results if we add noise to the data. These results indicate that the incremental approach is a promising method for this class of transport identification problems.

The paper is organized as follows. The incremental approach of modeling and identification of transport phenomena is presented in Section 2. The optimization-based formulations for the inverse problems arising in the first two steps of the identification procedure and the parameter estimation problem for the transport model in the third step are given in Section 3. In that section, we also describe the conjugate gradient solution method based on adjoint problems for gradient computation, which we use to solve the inverse problem arising in the first step of the incremental identification. We give the description of the inexact Newton-type method with which we solve the more complicated nonlinear inverse problem in the second step, as well. In Section 4 we present results of extensive numerical experiments for the identification of a model for the transport coefficient in a three-dimensional convection-diffusion problem of type (1.1). This model problem is motivated by research on energy transport in wavy films, using effective transport coefficients [8, 12, 32]. Section 5 contains some conclusions and remarks concerning future work.

2. Incremental modeling and identification. The key idea of the incremental approach is the gradual refinement of the model structure during identification, reflecting the incremental steps which are common in model development. The main steps of model development and their relation to incremental model identification are outlined in the following.

2.1. Incremental modeling. Incremental modeling aims at a generic and structured process for the development of model equations [23, 24]. The starting point is the formulation of the balance equations. The balance equation for a scalar state $u(\mathbf{x}, t)$, that denotes the specific quantity conserved, is given by

$$\frac{\partial \rho u}{\partial t} + \nabla \cdot \mathbf{j} = 0\,.$$

Here, $\mathbf{j}$ is the flux vector, that governs the rate of transfer of the conserved physical quantity. This vector consists of a convective and diffusive part:

$$\mathbf{j} = \rho u \mathbf{w} + \mathbf{q}\,.$$

The use of the continuity equation

$$\frac{\partial \rho}{\partial t} + \nabla \cdot \rho \mathbf{w} = 0\,,$$

leads to the convection-diffusion equation

$$\text{model } B\text{:} \qquad \frac{\partial u}{\partial t} + \mathbf{w} \cdot \nabla u = -\frac{1}{\rho} \nabla \cdot \mathbf{q} \quad \text{in } \Omega \times (t_0, t_f]\,. \tag{2.1}$$

We do not refine this equation any further, i. e. at this decision level no additional assumptions are made about the potentially uncertain constitutive relation for the diffusive flux vector $\mathbf{q}$.

In the next step, the model is refined by specifying a functional form of the flux $\mathbf{q}$. Often a constitutive relation is used, for example, Fourier's law in heat transfer or Fick's law in mass transfer, which can be cast as

$$\text{model } F\text{:} \qquad \mathbf{q} = -a \nabla u \quad \text{in } \Omega \times (t_0, t_f]\,, \tag{2.2}$$

with an unknown transport coefficient a. In empirical approaches one usually distinguishes different transport mechanisms, namely transport by turbulent or molecular mechanisms, with or without convection [10]. Accordingly, the transport coefficient in (2.2) is represented as a sum of two contributions - the *known* molecular part a_{mol}, the *molecular transport coefficient* corresponding to molecular transport (e. g. heat conduction through the fluid) and the *unknown* remaining part $a_w(\mathbf{x}, t)$ capturing the remaining transport effects (e. g. due to turbulence or other transport enhancing effects). In the following, we call $a_w(\mathbf{x}, t)$ the *enhanced transport coefficient*. Thus,

$$a(\mathbf{x}, t) = a_{\mathrm{mol}} + a_w(\mathbf{x}, t)\,, \quad (\mathbf{x}, t) \in \Omega \times [t_0, t_f]\,. \tag{2.3}$$

Consequently the flux law (2.2) can be written as

$$\mathbf{q} = -(a_{\mathrm{mol}} + a_w) \nabla u \quad \text{in } \Omega \times (t_0, t_f]\,. \tag{2.4}$$

In the final step of the incremental modeling procedure, a further refinement level is added by specifying a constitutive relation for the enhanced transport coefficient to close the model. We formulate it in a generic way,

$$\text{model } T\text{:} \qquad a_w(\mathbf{x}, t) = f_{\mathrm{w}}(u(\mathbf{x}, t), \mathbf{x}, t, \theta)\,, \tag{2.5}$$

to correlate a_w with the state u and model parameters $\theta \in \mathbb{R}^n$.

2.2. Incremental identification. The incremental identification directly follows the steps of model development [24]. We assume throughout, that appropriate transient measurement data at sufficiently high resolution in space $\mathbf{x}$ and time t are available. A schematic picture of the procedure is given in Fig. 1.

We rewrite the balance equation (2.1) as

$$\frac{\partial u}{\partial t} + \mathbf{w} \cdot \nabla u = F \quad \text{in } \Omega \times (t_0, t_f]\,, \tag{2.6}$$

with

$$F(\mathbf{x}, t) = -\nabla \cdot \mathbf{q}(\mathbf{x}, t)\,, \quad (\mathbf{x}, t) \in \Omega \times (t_0, t_f]\,. \tag{2.7}$$

Here, we have assumed for simplicity a constant density normalized to $\rho = 1$. In the first step of the incremental identification procedure, the (artificial) *source* $F(\mathbf{x}, t)$ is estimated, as a function of space and time, from the balance equation (2.6) with

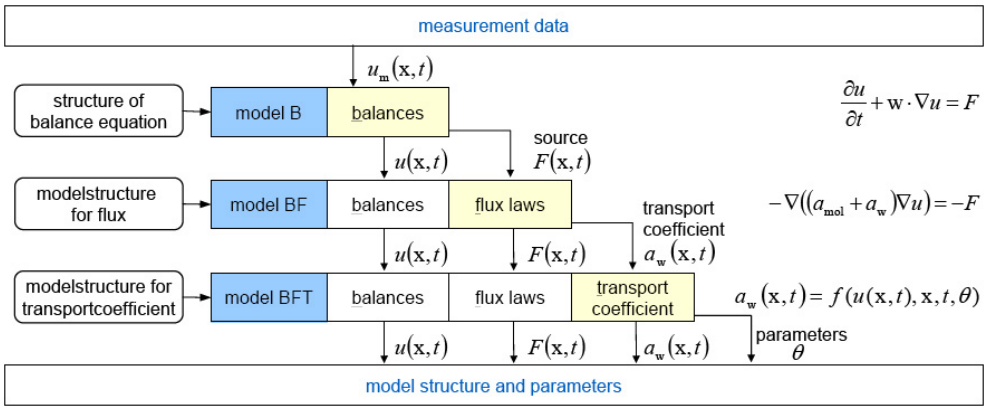

FIG. 1. *Incremental modeling and identification of transport phenomena.*

proper initial and boundary conditions, on the basis of suitable measurements $u_m(\mathbf{x}, t)$ of the state $u(\mathbf{x}, t)$. This is a typical example of a *source inverse problem* [2].

The incremental identification at the next level uses the estimated source $F(\mathbf{x}, t)$ as model-based measurement data together with the transient measurements $u_m(\mathbf{x}, t)$ to reconstruct the transport coefficient $a_w(\mathbf{x}, t)$. Hence $a_w(\mathbf{x}, t)$ is to be estimated from the equation

$$-\nabla \cdot ((a_{\mathrm{mol}} + a_w)\, \nabla u) = -F \quad \text{in } \Omega \times (t_0, t_f]\,, \tag{2.8}$$

which corresponds to a *coefficient inverse problem* [2].

In the third step of the identification procedure the reconstructed coefficient $a_w(\mathbf{x}, t)$ is correlated with states as in (2.5) by solving a parameter estimation problem. Different model candidates involving the state u and model parameters θ can be considered here. The measurement data are used to estimate parameters for each candidate model. The best model is selected by carrying out a model discrimination between candidates using some measure of model validity [31].

In this paper, we focus on the inverse problems that arise in the first two steps of the incremental identification approach. In the third identification step we estimate model parameters in a model structure for the transport coefficient which is assumed to be known. In this paper, we restrict ourselves to the estimation of one given model for the transport coefficient, i. e., we do not yet consider the discrimination issue between competing model candidates.

For the numerical treatment of the source inverse problem in the first step it is very convenient to consider a variant of (2.6) which uses the expression (2.8) for the transport coefficient. This leads to

$$F(\mathbf{x}, t) = \nabla \cdot (a_{\mathrm{mol}} \nabla u(\mathbf{x}, t)) + F_w(\mathbf{x}, t)\,, \quad (\mathbf{x}, t) \in \Omega \times [t_0, t_f]\,. \tag{2.9}$$

As a result, instead of $F(\mathbf{x}, t)$ it suffices to estimate the enhanced part $F_w(\mathbf{x}, t)$ of the source term on the basis of transient measurement data $u_m(\mathbf{x}, t)$. Consequently, in the first step of the identification procedure one has to reconstruct the source term $F_w(\mathbf{x}, t)$ in the following *convection-diffusion* equation

$$\text{model } \overline{B}\text{:} \qquad \frac{\partial u}{\partial t} + \mathbf{w} \cdot \nabla u - \nabla \cdot (a_{\mathrm{mol}} \nabla u) = F_w \quad \text{in } \Omega \times (t_0, t_f]\,, \tag{2.10a}$$

with initial and boundary conditions

$$\begin{aligned} u(\mathbf{x},t_0) &= u_0(\mathbf{x})\,,\ \mathbf{x}\in\Omega\,,\\ u(\mathbf{x},t) &= g_D(\mathbf{x},t)\,,\ (\mathbf{x},t)\in\Gamma_D\times[t_0,t_f]\,,\\ \frac{\partial u}{\partial n}(\mathbf{x},t) &= g_N(\mathbf{x},t)\,,\ (\mathbf{x},t)\in\Gamma_N\times[t_0,t_f]\,. \end{aligned} \tag{2.10b}$$

Compared to (2.6), we now have a convection-diffusion problem instead of a pure convection problem. Due to the diffusion part, the numerical treatment becomes easier. Furthermore, for u we can now use the same boundary conditions as in (1.1b).

In the second step of the incremental identification procedure, one has to determine the coefficient $a_w(\mathbf{x},t)$ in the diffusion equation,

$$\text{model } \overline{F}\text{:}\qquad -\nabla\cdot(a_w^t\nabla u^t) = -F_w^t \quad \text{in } \Omega\,, \tag{2.11a}$$

with boundary conditions

$$\begin{aligned} u^t(\mathbf{x}) &= g_D^t(\mathbf{x})\,,\quad \mathbf{x}\in\Gamma_D\,,\\ \frac{\partial u^t}{\partial n}(\mathbf{x}) &= g_N^t(\mathbf{x})\,,\quad \mathbf{x}\in\Gamma_N\,. \end{aligned} \tag{2.11b}$$

Here, for a space and time dependent function $\xi(\mathbf{x},t)$ we have introduced the notation $\xi^t(\mathbf{x}) := \xi(\mathbf{x},t)\,,(\mathbf{x},t)\in\Omega\times[t_0,t_f]$ to decouple the function values in time instants. In (2.11) we thus have a *stationary* diffusion problem for each given $t\in[t_0,t_f]$.

In the third step of the identification procedure, the reconstructed coefficients $a_w^t(\mathbf{x})$ at selected times $t\in[t_0,t_f]$ have to be correlated with states $u^t(\mathbf{x})$ and parameters θ in the parametric model

$$\text{model } \overline{T}\text{:}\qquad a_w^t(\mathbf{x}) = f_{\mathrm{w}}(u^t(\mathbf{x}),\mathbf{x},t,\theta)\,. \tag{2.12}$$

We briefly compare the incremental identification approach to the established simultaneous identification approach. For this purpose, we insert the relation (2.5) into the flux model and insert the result into the convection-diffusion equation (1.1a),

$$\text{model } \overline{BFT}\text{:}\qquad \frac{\partial u}{\partial t} + \mathbf{w}\cdot\nabla u - \nabla\cdot(f(u(\mathbf{x},t),\mathbf{x},t,\theta)\nabla u) = 0 \quad \text{in } \Omega\times(t_0,t_f]\,, \tag{2.13a}$$

with initial and boundary conditions

$$\begin{aligned} u(\mathbf{x},t_0) &= u_0(\mathbf{x})\,,\quad \mathbf{x}\in\Omega\,,\\ u(\mathbf{x},t) &= g_D(\mathbf{x},t)\,,\quad (\mathbf{x},t)\in\Gamma_D\times[t_0,t_f]\,,\\ \frac{\partial u}{\partial n}(\mathbf{x},t) &= g_N(\mathbf{x},t)\,,\quad (\mathbf{x},t)\in\Gamma_N\times[t_0,t_f]\,. \end{aligned} \tag{2.13b}$$

While the incremental approach decomposes the identification process for the transport coefficient in three steps, in the simultaneous approach the models for the flux (e.g. (2.2)) and for the transport coefficient (e.g. (2.5)) are collected in one equation (2.13a). Hence, all the assumptions made during the modeling will simultaneously influence the identification. Due to this, the level of uncertainty of the simultaneous problem (2.13) has increased, leading to a higher risk of poor estimates.

A further advantage of the incremental approach is that, for known velocity $\mathbf{w}(\mathbf{x},t)$ and molecular transport coefficient a_{mol}, it suffices to reconstruct the source $F_w(\mathbf{x},t)$ at the first level and the enhanced transport coefficient $a_w(\mathbf{x},t)$ at the second level only *once*. The complexity due to the elimination of candidate models for the transport coefficient affects the third (final) level *only*, thus allowing for a more systematic derivation of suitable candidate models.

Compared to the simultaneous problem (2.13), where a nonlinear coefficient inverse problem in space and time has to be solved, the incremental identification procedure has advantages from the optimization point of view. The reconstruction of the source in the first step results in a *dynamic* optimization problem, which is *affine-linear* in the unknown. The latter property implies that (compared to a strongly nonlinear case) relatively simple and efficient optimization methods can be applied. In the second step of the identification, we have to deal with a nonlinear coefficient inverse problem which, however, is of *steady-state* type for each given time t, cf. (2.11). In this sense the incremental approach decouples dynamics and nonlinearity, which has advantages for the numerical treatment of nonlinear inverse problems for evolution equations in three dimensions. Furthermore, the - in the worst case - combinatorial problem of identifying a suitable model structure is decoupled from the problem of inversion of differential equations.

The estimation problems arising in the first two steps of the incremental approach are typical inverse problems, ill-posed by nature. This raises, however, the question of error propagation through the sequence of inverse problems. This issue is studied for the illustrative model problem in Section 4.

3. Formulation and solution of the inverse problems. The inverse problems resulting in the three incremental steps are formulated as optimization problems [1, 2, 25].

In the first step of the incremental identification procedure, the source F_w should minimize the quadratic objective functional

$$J_1(F_w) = \frac{1}{2}\int_{t_0}^{t_f}\int_{\Omega}\left[u(\mathbf{x},t;F_w) - u_m(\mathbf{x},t)\right]^2 \, d\mathbf{x}\, dt\,, \tag{3.1}$$

with suitable transient measurement data $u_m(\mathbf{x},t)\,,(\mathbf{x},t)\in\Omega\times[t_0,t_f]$. Here $u(\mathbf{x},t;F_w)$ is the solution of the *direct problem* (2.10) with known initial condition u_0 and boundary conditions g_D and g_N. We use the notation $u(\mathbf{x},t;F_w)$ to emphasize the dependence of the function u on the unknown source F_w.

Similarly, the second identification step concerns the estimation of the enhanced transport coefficients $a_w^t(\mathbf{x})$ as a functions of space $\mathbf{x}$ at selected times $t\in[t_0,t_f]$, using the previously estimated source $F_w^t(\mathbf{x})$ and the measurement data $u_m^t(\mathbf{x})$. The optimization-based formulation of this coefficient inverse problem consists of the minimization of the objective functional

$$J_2(a_w^t) = \frac{1}{2}\int_{\Omega}\left[u^t(\mathbf{x};a_w^t) - u_m^t(\mathbf{x})\right]^2 \, d\mathbf{x}\,. \tag{3.2}$$

Here $u^t(\mathbf{x};a_w^t)$ denotes the solution of the direct problem (2.11) for given a_w^t.

Finally, in the third identification step, the reconstructed transport coefficients $a_w^t(\mathbf{x})$ at times $t\in[t_0,t_f]$ are further used in order to find the parametric model $f(u^t(\mathbf{x}),\mathbf{x},t,\theta)$, $\theta\in\mathbb{R}^n$ (cf. (2.12)). We formulate this problem as a standard least-

squares problem, such that the model $f(\,\cdot\,)$ minimizes the objective functional

$$J_3(f(u^t(\mathbf{x}),\mathbf{x},t,\theta)) = \frac{1}{2}\sum_t \int_\Omega \left[a_w^t(\mathbf{x}) - f(u^t(\mathbf{x}),\mathbf{x},t,\theta)\right]^2 \, d\mathbf{x}\,. \tag{3.3}$$

This estimation problem depends strongly on the availability of candidate models $f(\,\cdot\,)$. In cases where no reasonable (structured) model can be formulated (i.e. the model structure is unknown) a general parameterization capable of approximating functions from a sufficiently large class should be introduced for the transport coefficient a_w and the model parameters θ should be estimated by means of data-driven techniques [21]. In case of (structured) available model candidates, e.g. from physical considerations and/or *a priori* knowledge, the parameters θ are to be estimated for *each* candidate model. Subsequently, the adequacy of the different candidates has to be quantified with the use of model discrimination approaches in order to choose the best model for the transport coefficient [31].

3.1. Numerical solution strategy. For the solution of the optimization problem in the first step of the incremental approach, the conjugate gradient method is used [15, 25]. The optimization problem in the second step is solved by means of an inexact Newton-type method, which is an appropriate technique for a large class of nonlinear inverse problems [14]. In this paper, regularization is only introduced via spatial and temporal discretization and by means of a suitable stopping criterion for the optimization algorithms. Hence, for a given fixed discretization, the number of optimization iterations serves as a regularization parameter [14]. Either the heuristic L-curve method [20] or the discrepancy principle [14] is used to determine an appropriate value of this parameter.

In the following subsections we assume H to be a given (Hilbert) space with scalar product $(\cdot,\cdot)_H$ and corresponding norm $\|\cdot\|_H^2 = (\cdot,\cdot)_H$.

3.1.1. Estimation of the source $F_w(\mathbf{x},t)$. For the minimization of the objective functional (3.1) with constraints (2.10) the conjugate gradient (CG) method is used [1]. The algorithmic structure is as follows:

(i) Set $n \leftarrow 0$ and choose an initial guess $F_w^0 \in H$.

(ii) If the objective function satisfies a given tolerance criterion, stop, otherwise continue .

(iii) Calculate the new search direction as

$$\tilde{F}_w^n = \nabla J_1(F_w^n) + \gamma^n \tilde{F}_w^{n-1}\,, \tag{3.4a}$$

with

$$\gamma^n = \frac{\|\nabla J_1(F_w^n)\|_H^2}{\left\|\nabla J_1(F_w^{n-1})\right\|_H^2}, \quad \text{for} \quad n \geq 1 \quad \text{and} \quad \gamma^0 := 0\,, \tag{3.4b}$$

(iv) Calculate a step length μ by solving a one-dimensional minimization problem resulting in

$$\mu^n = \frac{\left(u_m - u(F_w^n),\, S_1(\tilde{F}_w^n)\right)_H}{\left\|S_1(\tilde{F}_w^n)\right\|_H^2}\,, \tag{3.5}$$

with $u(F_w^n)$ the solution of the direct problem (2.10) and S_1 the solution of the *sensitivity problem* (3.7) below.

(v) Update the approximation according to

$$F_w^{n+1} = F_w^n + \mu^n \tilde{F}_w^n \,. \tag{3.6}$$

(vi) Set $n \leftarrow n+1$ and repeat the procedure starting with (ii).

In the CG method, one has to calculate the gradient of the objective functional $\nabla J_1(F_w^n)$. This gradient can be determined from the solution of an *adjoint problem*. The calculation of the step length in (iv) requires the solution of the *sensitivity problem*. We do not give a derivation of the adjoint and the sensitivity problems, since this can be found in the literature, e.g. [1].

The sensitivity problem corresponding to (2.10) is given by

$$\frac{\partial S_1}{\partial t} + \mathbf{w} \cdot \nabla S_1 - a_{\mathrm{mol}} \Delta S_1 = \tilde{F}_w \quad \text{in } \Omega \times (t_0, t_f] \,, \tag{3.7a}$$

$$\begin{aligned} S_1(\mathbf{x}, t_0) &= 0 \,, \quad \mathbf{x} \in \Omega \,, \\ S_1(\mathbf{x}, t) &= 0 \,, \quad (\mathbf{x}, t) \in \Gamma_D \times [t_0, t_f] \,, \\ \frac{\partial S_1}{\partial n}(\mathbf{x}, t) &= 0 \,, \quad (\mathbf{x}, t) \in \Gamma_N \times [t_0, t_f] \,. \end{aligned} \tag{3.7b}$$

where $\tilde{F}_w(\mathbf{x}, t)$ is a perturbation of the unknown source F_w. This partial differential equation has exactly the same structure as the corresponding direct problem (2.10), only the initial and boundary conditions are different.

It can be shown that the gradient of the objective functional satisfies

$$\nabla J_1(F_w) = \varphi_1 \quad \text{in } \Omega \times [t_0, t_f] \,, \tag{3.8}$$

where the adjoint variable φ_1 is the solution of the adjoint problem

$$-\frac{\partial \varphi_1}{\partial t} - \mathbf{w} \cdot \nabla \varphi_1 - a_{\mathrm{mol}} \Delta \varphi_1 = [u(F_w) - u_m] \quad \text{in } \Omega \times [t_0, t_f) \,, \tag{3.9a}$$

$$\begin{aligned} \varphi_1(\mathbf{x}, t_f) &= 0 \,, \quad \mathbf{x} \in \Omega \,, \\ \varphi_1(\mathbf{x}, t) &= 0 \,, \quad (\mathbf{x}, t) \in \Gamma_D \times [t_0, t_f] \,, \\ \frac{\partial \varphi_1}{\partial n}(\mathbf{x}, t) &= 0 \,, \quad (\mathbf{x}, t) \in \Gamma_N \times [t_0, t_f] \,. \end{aligned} \tag{3.9b}$$

In contrast to the direct problem (2.10), we now have a condition at final time t_f. We do not give the derivation of the identity (3.8) since it follows from a standard procedure, cf. [1]. Going backwards in time (by introducing a new time variable $t_f - t$), equation (3.9) shows exactly the same structure as the direct problem (2.10), only with different initial and boundary conditions.

Thus, the CG algorithm for minimizing J_1 requires the solution of three very similar problems in every iteration, namely the direct, the adjoint and the sensitivity problem. However, due to the linearity of the involved equations only *two* problems - the sensitivity (3.7) and the adjoint (3.9) problem - have to be solved. Instead of solving the direct problem (2.10) for $u(\mathbf{x}, t; F_w)$, the linear update formula

$$u(F_w^{n+1}) = u(F_w^n) + \mu_1^n S_1(\tilde{F}_w^n) \tag{3.10}$$

can be applied.

In [17] we have considered a similar inverse problem, where a boundary heat flux in a nonstationary three-dimensional heat conduction problem has been estimated from boundary temperature measurements in a falling film experiment. The solution strategy presented there is of the same type as the source estimation described above.

3.1.2. Estimation of the transport coefficients $a_w^t(\mathbf{x})$. For the minimization of the objective functional (3.2) with constraints (2.11) a Newton-type method is used. The basic idea is the computation of a regularized approximation of the linearized problem by an *inner iteration*, namely a CG method [18]. In case of inexact data the regularizing effect of this algorithm comes, in analogy to the CG method above, from appropriate termination of the iteration.

The general framework of the *truncated Newton-CGNE* method [18] is as follows:

(i) Set $k \leftarrow 0$ and choose an initial guess $a_w^{t\,0} \in H$.

(ii) If the objective function satisfies a given tolerance criterion, stop, otherwise continue .

(iii) Choose values $n_\star > 1$ and $\eta \in (0,1)$ and set

$$\begin{aligned} n &\leftarrow 0\,, \\ y &= u_m^t - u(a_w^{t\,k})\,, \\ r^0 &= y\,, \\ x^0 &= 0\,, \end{aligned}$$

with $u(a_w^{t\,k})$ the solution of the direct problem (2.11).

(iv) **repeat** (inner CG iteration)

(a) Calculate the new search direction as

$$\tilde{a}_w^{t\,n} = \varphi_2(a_w^{t\,k}, r^n) + \beta^n \tilde{a}_w^{t\,n-1}\,, \tag{3.11a}$$

with

$$\beta^n = \frac{\left\|\varphi_2(a_w^{t\,k}, r^n)\right\|_H^2}{\left\|\varphi_2(a_w^{t\,k}, r^{n-1})\right\|_H^2}, \quad \text{for} \quad n \geq 1 \quad \text{and} \quad \beta^0 := 0\,, \tag{3.11b}$$

where φ_2 denotes the solution of an *adjoint problem* (see (3.17) below).

(b) Calculate the optimal step length for the linearized problem by

$$\alpha^n = \frac{\left(r^n, S_2(a_w^{t\,k}, \tilde{a}_w^{t\,n})\right)_H}{\|S_2(a_w^{t\,k}, \tilde{a}_w^{t\,n})\|_H^2}\,, \tag{3.12}$$

with S_2 the solution of a *sensitivity problem* (see (3.16) below).

(c) Update the inner iteration according to

$$x^{n+1} = x^n + \alpha^n \tilde{a}_w^{t\,n}\,, \tag{3.13a}$$

$$r^{n+1} = r^n - \alpha^k S_2(a_w^{t\,k}, \tilde{a}_w^{t\,n})\,. \tag{3.13b}$$

(d) Set $n \leftarrow n+1$.

until the stopping criterion

$$\|r^n\| < \eta\,\|y\| \quad \text{or} \quad n \geq n_\star \tag{3.14}$$

is satisfied.

(v) Update the approximation according to

$$a_w^{t\,k+1} = a_w^{t\,k} + x^n\,. \tag{3.15}$$

(vi) Set $k \leftarrow k+1$ and repeat the procedure starting with (ii).

According to the stopping rule (3.14) for the inner iteration, this method belongs to the general class of *inexact Newton methods* [25]. Besides this stopping rule, the difference between the inner iteration and the CG algorithm above is, that the gradient of the objective functional ∇J_1 is replaced by φ_2 - the solution of a different adjoint problem. It should be emphasized here that, for the nonlinear problems the relation similar to (3.8) does not hold, cf. e.g. [2]. In the truncated Newton-CGNE method, one has to solve an adjoint and a sensitivity problem in every inner iteration in addition to the direct problem in every outer iteration. Due to the nonlinearity of the estimation problem, a simple update formula similar to (3.10) is not available. The adjoint and the sensitivity problems for the minimization of the functional (3.2) with constraints (2.11) are stated next (for the derivation see e.g. [2]).

The sensitivity problem is given by

$$-\nabla \cdot (a_w^t \nabla S_2^t) = \nabla \cdot (\tilde{a}_w^t \nabla u^t) \quad \text{in } \Omega\,, \tag{3.16a}$$

$$\begin{aligned} S_2^t(\mathbf{x}) &= 0\,, \quad \mathbf{x} \in \Gamma_D\,, \\ \frac{\partial S_2^t}{\partial n}(\mathbf{x}) &= 0\,, \quad \mathbf{x} \in \Gamma_N\,, \end{aligned} \tag{3.16b}$$

for each time $t \in [t_0, t_f]$. $S_2^t = S_2^t(\mathbf{x}; a_w^t, \tilde{a}_w^t)$ is the first order perturbation of the function $u^t(\mathbf{x}; a_w^t)$ caused by a perturbation $\tilde{a_w^t}(\mathbf{x})$ of the enhanced transport coefficient $a_w^t(\mathbf{x})$. $u^t = u^t(\mathbf{x}; a_w^t)$ in (3.16a) denotes the solution of the corresponding direct problem (2.11) for a given value of $a_w^t(\mathbf{x})$. This equation has the same structure as the corresponding direct problem. Note, however, that apart from the different boundary conditions one also has a specific right-hand side in this sensitivity equation, which arises due to the nonlinearity of the coefficient inverse problem.

The adjoint variable φ_2^t at time t is the solution of the adjoint problem

$$-\nabla \cdot (a_w^t \nabla \varphi_2^t) = [u^t(\mathbf{x}; a_w^t) - u_m^t(\mathbf{x})] \quad \text{in } \Omega\,, \tag{3.17a}$$

$$\begin{aligned} \varphi_2^t(\mathbf{x}) &= 0\,, \quad \mathbf{x} \in \Gamma_D\,, \\ \frac{\partial \varphi_2^t}{\partial n}(\mathbf{x}) &= 0\,, \quad \mathbf{x} \in \Gamma_N\,. \end{aligned} \tag{3.17b}$$

This problem has the same structure as the direct problem (2.11).

3.1.3. Solution of the PDE problems. All resulting direct, sensitivity and adjoint problems used in either of the optimization methods described above are either of elliptic or parabolic (convection-diffusion) type. Hence, similar numerical techniques can be employed for their solution. The three convection-diffusion problems (2.10), (3.7), (3.9) as well as the three steady-state diffusion problems (2.11), (3.16), (3.17) are solved with the same software code in case of source and coefficient estimation, respectively.

The solutions of all three 3D problems are calculated by means of the software package DROPS [13]. DROPS is based on multi-level nested grids and conforming finite element discretization methods. For time discretization a standard one-step θ-method is used. For the space discretization piecewise linear finite elements on a tetrahedral grid are employed. The resulting discrete systems of linear equations are solved by suitable Krylov subspace methods. In case of the convection-diffusion equations (2.10), (3.7), (3.9) we use a preconditioned Generalized Minimal Residuals (GMRES) method. For the diffusion problems (2.11), (3.16), (3.17) a preconditioned conjugate gradient (PCG) method is applied [29]. For the simulations presented in

this paper the SSOR method is used for preconditioning. Other options, for example multigrid solvers, are available in DROPS. In this paper we do not study efficiency of these solvers for the direct, the sensitivity and the adjoint problems. We use a fixed (quasi-uniform) mesh for discretization and prescribe a tolerance with which the discrete linear systems are solved.

3.1.4. Identification of a transport model $f(u^t(\mathbf{x}), \mathbf{x}, t, \theta)$. For the solution of an unconstrained minimization problem (3.3) in the final step of the incremental identification procedure, we use standard solution techniques for least-squares problems [25]. In our case study (cf. Section 4), we only consider a single model candidate for the transport coefficient, hence implicitly assuming that the model structure is known.

4. Illustrative case study. In this section, the incremental approach is illustrated for a problem motivated by the identification of energy transport in laminar wavy film flows. The complex dynamics of the nonlinear surface waves typically present in film flows [16, 26] renders a direct transient simulation in 3D numerically very complicated and computationally expensive. Therefore, manageable *approximate* descriptions, yet accurately modeling the underlying transport processes, have gained increasing importance in the engineering literature to support the design of technical systems [8]. A possible simplified model is as follows. In order to reduce the problem complexity, the 3D time-varying domain Ω_W corresponding to the liquid phase is mapped to a 3D time-invariant waveless domain $\Omega := (0, L_x) \times (0, L_y) \times (0, L_z) \subset \mathbb{R}^3$. This reduction is compensated by the introduction of a space- and time-dependent *effective* transport coefficient $a_{\text{eff}}(\mathbf{x}, t)$ [8, 12, 32] to capture all wave-induced transport effects in this flat film geometry.

Such a flat film model is considered in the remainder. It consists of a convection-diffusion system which describes energy transport in a single component fluid on the flat (rectangular) domain Ω with boundary $\Gamma = \partial\Omega$, with parts $\Gamma = \Gamma_{in} \cup \Gamma_{wall} \cup \Gamma_{out} \cup \Gamma_r$ defined as

$$\begin{aligned}
\Gamma_{in} &= \{(x, y, z) \in \Gamma : \ x = 0\} \subset \Gamma_D - \text{ the inflow boundary}, \\
\Gamma_{wall} &= \{(x, y, z) \in \Gamma : \ y = 0\} \subset \Gamma_D - \text{ the wall boundary}, \\
\Gamma_{out} &= \{(x, y, z) \in \Gamma : \ x = L_x\} \subset \Gamma_N - \text{ the outflow boundary}, \\
\Gamma_r &= \Gamma \setminus (\Gamma_{in} \cup \Gamma_{wall} \cup \Gamma_{out}) \subset \Gamma_N - \text{ the remaining boundaries}.
\end{aligned}$$

The state variable $u(\mathbf{x}, t)$ in (1.1) is the temperature $T(\mathbf{x}, t)$ and the transport coefficient $a(\mathbf{x}, t)$ is the *effective thermal diffusivity* $a_{\text{eff}}(\mathbf{x}, t)$. The unit cube $\Omega = (0, 1)^3[mm^3]$ is considered as computational domain for simplicity of presentation and to avoid possible numerical complications due to anisotropy effects. x corresponds to the flow direction of the falling film and y is the direction along the film thickness. The velocity $\mathbf{w}(\mathbf{x}, t)$ is given by a Nusselt-profile, i.e. $\mathbf{w}(\mathbf{x}, t) = 4.2857(2y - y^2)$ [27]. The initial condition is a constant, i.e. $T(\mathbf{x}, 0) = 15°C\,, \mathbf{x} \in \Omega$. The known Dirichlet boundary conditions are chosen as follows. The inflow temperature has a linear profile in y and drops from $15°C$ to $0°C$ along the y axis over time, i.e.

$$T_{in}(\mathbf{x}, t) = -30yt + 15\,, \quad (\mathbf{x}, t) \in \Gamma_{in} \times [t_0, t_f]\,. \tag{4.1a}$$

The wall temperature has a nonlinear profile in x and increases from $15°C$ to $65°C$ along the x axis over time, i.e.

$$T_{wall}(\mathbf{x}, t) = 100 \left(1 - \cos\left(\frac{\pi}{2}x\right)\right) t + 15\,, \quad (\mathbf{x}, t) \in \Gamma_{wall} \times [t_0, t_f]\,. \tag{4.1b}$$

At the Neumann boundaries Γ_{out} and Γ_r a zero diffusive flux condition is used, i.e.

$$\frac{\partial T}{\partial n}(\mathbf{x},t) = 0\,, \quad (\mathbf{x},t) \in (\Gamma_{out} \cup \Gamma_r) \times [t_0, t_f]\,. \tag{4.1c}$$

The effective thermal diffusivity a_{eff} is chosen to have a sinusoidal pattern over the space coordinate in the flow direction of the falling film (i.e. the $x-$direction). The wavy pattern is assumed to be time-dependent, such that the waves travel along the x-direction starting from a constant value at the inflow boundary Γ_{in} (i.e. $x = 0\,mm$). They propagate along the $y-$ and $z-$directions with a larger gradient in the y-direction (film thickness) starting from a constant value at the wall boundary Γ_{wall} (i.e. $y = 0\,mm$), and with a comparably low gradient in the z-direction:

$$a_{\text{eff}}(\mathbf{x},t) = a_{\text{mol}} + a_w(\mathbf{x},t)\,, \tag{4.2a}$$

$$a_w(\mathbf{x},t) = 5\left(1.1 + \frac{y}{5}\left(\sin\left(\pi x + \frac{t}{50}\right) + x + \frac{xz}{10}\right)\right)\,, \tag{4.2b}$$

$$(x,y,z,t) \in \Omega \times [t_0, t_f]\,.$$

The material properties of the fluid are lumped in the known constant *molecular thermal diffusivity* $a_{\text{mol}} = 0.35\frac{mm^2}{s}$, whereas the remaining part of the effective thermal diffusivity $a_{\text{eff}}(\mathbf{x},t)$ represents the unknown *wavy thermal diffusivity* $a_w(\mathbf{x},t)$, the transport coefficient capturing the wave-induced effects in the flat film model.

In this setting, a model $f_{\text{w}}(\mathbf{x},t,\theta)$ (cf. (2.5)) for the "true" wavy thermal diffusivity $a_w(\mathbf{x},t)$ in (4.2b) can be formulated as

$$f_{\text{w}}(\mathbf{x},t,\theta) = 5\left(\vartheta_1 + \vartheta_2 y\left(\sin\left(\vartheta_3 x + \vartheta_4 t\right) + 0.2x + \vartheta_5 xz\right)\right)\,, \tag{4.3}$$

$$(x,y,z,t) \in \Omega \times [t_0, t_f]\,, \theta \in \mathbb{R}^5\,,$$

where the vector $\theta = (\vartheta_1, \ldots, \vartheta_5)$ represents the vector of model parameters. A comparison of (4.2b) and (4.3) reveals the true underlying value θ^{ex} of this vector to be

$$\theta^{ex} = (1.1, 0.2, \pi, 0.02, 0.1)\,. \tag{4.4}$$

In order to generate high quality temperature simulation data the nonlinear direct problem (2.13) with the "true" effective thermal diffusivity given in (4.2) is solved on a uniform fine grid with the spatial discretization consisting of $48 \times 48 \times 38$ intervals in $x\,, y$ and z directions, respectively. This yields a space discretization with 89856 unknowns and 525312 tetrahedra.

For the solution of the inverse problems in the first two steps as well as for the solution of the parameter estimation problem in the third step of the incremental identification, we use the temperature data T_m on the coarser grid of resolution $24 \times 24 \times 19$ intervals in $x\,, y$ and z directions, respectively, to avoid so-called "inverse crime" [22]. Furthermore, we assume to know the correct structure of the model. This assumption does not hold in a real problem setting, where an appropriate model structure has to be identified from the measurement data.

In the first step of the incremental identification procedure, we use the implicit Euler scheme with time step $\tau = 0.01s$ and apply 50 time steps starting from the initial time $t_0 = 0s$ (i.e. $t_f = 0.5s$). For the initial approximation in the optimization procedure, due to the lack of better information, we choose $F_w^0(\mathbf{x},t) = 0\,, (\mathbf{x},t) \in \Omega \times [0s, 0.5\,s]$.

In the second step of the incremental identification procedure, the same boundary conditions (cf. (4.1)) are used. The time interval $[0s, 0.5s]$ is subdivided in 50 time steps and the estimation of the wavy thermal diffusivity is carried out separately for each point in time. The initial time $t_0 = 0s$ is a singular point, because the initial temperature is constant and no reconstruction is possible, since the coefficient is not uniquely defined in this case (cf. (2.10)).

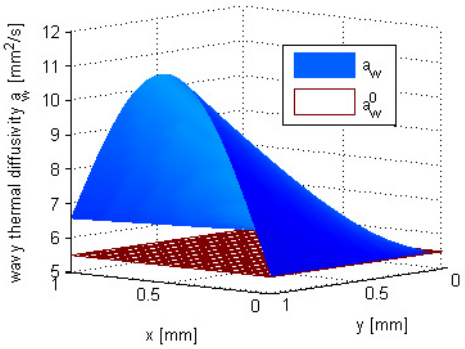

FIG. 1. *Initial approximation for the wavy thermal diffusivity* a_w^t *at* $t = 0.01s$ *and constant* $z = 0.5\,mm$.

As expected, the choice of a suitable initial vector for the optimization method is much more important for the *non*linear optimization problem in the second identification step than for the linear one in the first step. In our experiment, we use the constant

$$a_w^{t\,0} = 5.5 \tag{4.5}$$

as initial guess for the wavy thermal diffusivity in the first time step $t = 0.01s$ (cf. Fig. 1). This initial guess is very different from the true solution, but coincides with the inflow ($x = 0\,mm$) and wall ($y = 0\,mm$) boundary conditions Γ_D. The solution of the adjoint problem (3.17) is always zero along these boundaries - a direct consequence of the boundary conditions. From the truncated Newton-CGNE framework it follows, that in case $\varphi_2 = 0$ no update will be gained for the search direction in (3.11). As a consequence, the inner iteration can not be improved by the formula (3.13a). Subsequently, neither an update is possible in the outer iteration by (3.15). Hence, with such a choice of the initial approximation for the wavy thermal diffusivity we exclude from the estimation the boundaries where no information can be gained.

In the third step, the estimated functions $a_w^t(\mathbf{x})$ at time instants $t \in [0.01s, 0.5s]$, are used as model-based measurement data to estimate the model parameters $\theta \in \mathbb{R}^5$ of the model (4.3) by solving the standard least-squares problem (3.3). The initial guess $\theta^0 = (0.5, 0.5, 0.5, 0.5, 0.5)$ is chosen in all of our computations.

Estimation results with error-free measurements will be considered first. Subsequently the estimation with artificially perturbed measurements will be analysed.

4.1. Estimation with error-free measurements. In Fig. 2 (a) the objective functional $J_1(F_w)$ is plotted over the number of optimization iterations. In Fig. 2 (b), the source $F_w(\mathbf{x}, t)$ is plotted as a function of x for fixed $y = 0.5\,mm$ and $z = 0.5\,mm$ (i. e. at the middle of the $y-$ and $z-$domain, respectively) at a certain time for different numbers of optimization iterations denoted by *nopt*. Snapshots of the estimated

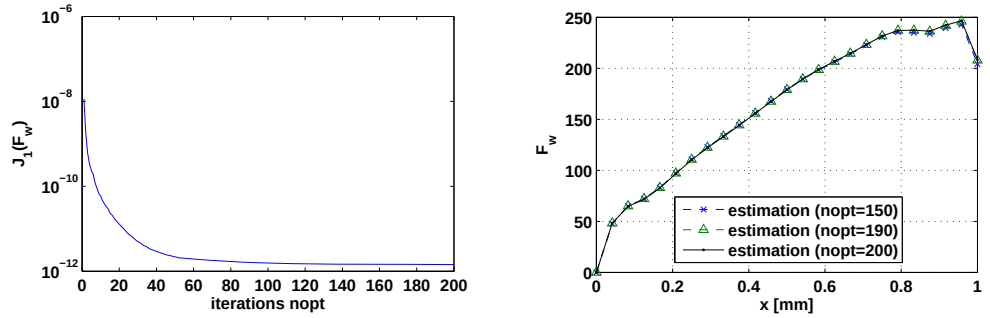

(a) (b)

FIG. 2. *(a) Objective functional J_1. (b) Estimated source F_w for different iterations nopt at time $t = 0.03s$, $y = 0.5\,mm$ and $z = 0.5\,mm$.*

source $F_w^{200}(\mathbf{x}, t)$ at the end of the optimization procedure ($nopt = 200$) are presented in Fig. 3. During the optimization the initial approximation at the boundaries Γ_{in} ($x = 0\,mm$) and Γ_{wall} ($y = 0\,mm$) could not be improved, since the gradient of the objective functional $J_1(F_w)$ is always zero along these boundaries. This follows directly from the boundary conditions of the corresponding adjoint problem (3.9) and the expression (3.8) for the gradient $\nabla J_1(F_w)$.

The estimation of the wavy thermal diffusivities $a_w^t(\mathbf{x})$ at times $t \in [0.01s, 0.5s]$ in the second step of the incremental approach, uses the estimated source $F_w^{200\,t}(\mathbf{x})$ at iteration $nopt = 200$ and the temperature $T_m^t(\mathbf{x})$ at given time t. We choose (4.5) as the initial approximation at time $t = 0.01s$. The subdivision in time gives a flexibility to improve this initial approximation at later times. Therefore, we use already computed estimates at time instants t as initial guesses for the next times $(t + \tau)$. Note, that the initial value for time $t = 0.01s$ restores the information lost at the inflow and wall boundaries at which the source $F_w(\mathbf{x}, t)$ could not be reconstructed in the first step.

The estimates of the wavy thermal diffusivity for $z = 0.5\,mm$ at selected times are shown in Fig. 4 (a), whereas Fig. 4 (b) shows contour lines of the differences between the exact and estimated quantities. The estimates in these figures have been obtained as follows. At time $t = 0.01s$, 100 Newton (outer) iterations were applied, whereas $\eta = 0.8$ and $n_\star = 50$ were used in the stopping rule (3.14) of the inner iteration. The analysis of the results for later times $t > 0.01s$ shows, that the solution converges already in 5 Newton iterations. Moreover, it is not necessary to require

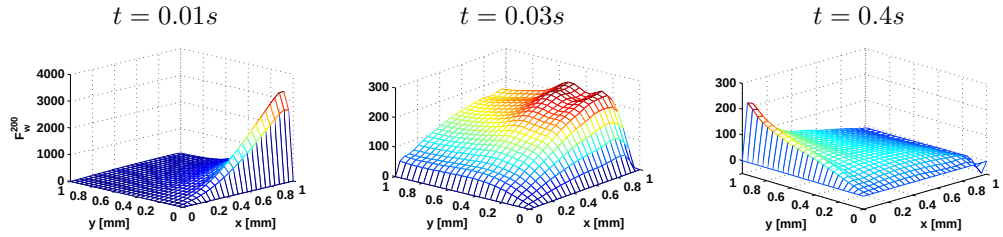

FIG. 3. *Estimated source F_w at different times for constant $z = 0.5\,mm$ with unperturbed measurements for nopt = 200.*

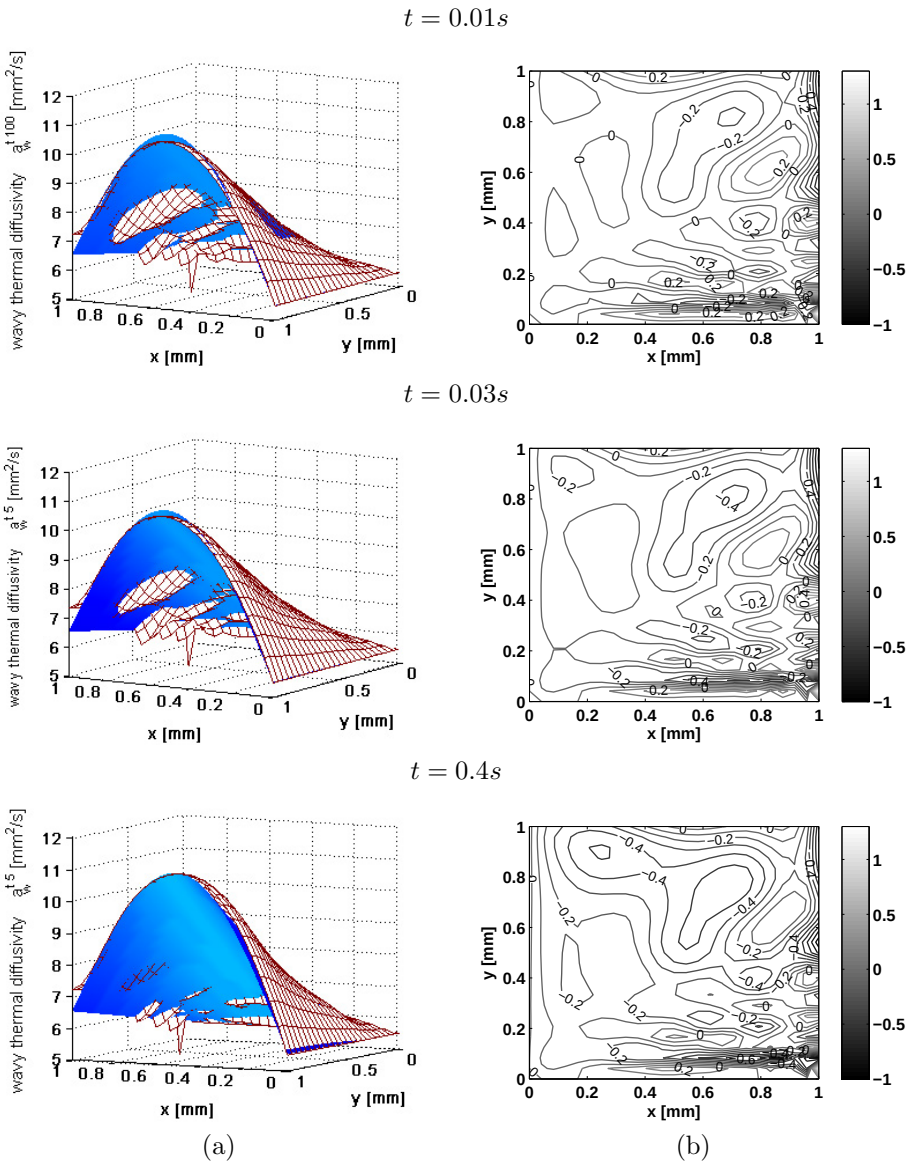

FIG. 4. *(a) Estimated (meshed surface) and exact (shaded surface) wavy thermal diffusivities a_w^t, (b) deviation between exact and estimated wavy thermal diffusivities a_w^t at different times.*

such a high number of inner iterations, because very good initial values are available at later times. We found the values of $\eta = 0.98$ and $n_\star = 20$ most favourable for times $t > 0.01s$.

A closer look at the results reveals that, independent of time, the estimation quality decreases in the x-direction (i.e. the direction of flow) by approaching the outflow boundary Γ_{out} (i.e. $x = 1\,mm$). This can be observed in Fig. 5, where the estimates are presented exemplarily for $t = 0.01s$ as a functions of y for $x \in \{0.2, 0.5, 1\}\,mm$ and $z = 0.5\,mm$. The development of the estimates for different numbers of Newton iterations *nopt* is shown in the figures, too. The reason of this distortion is, that at

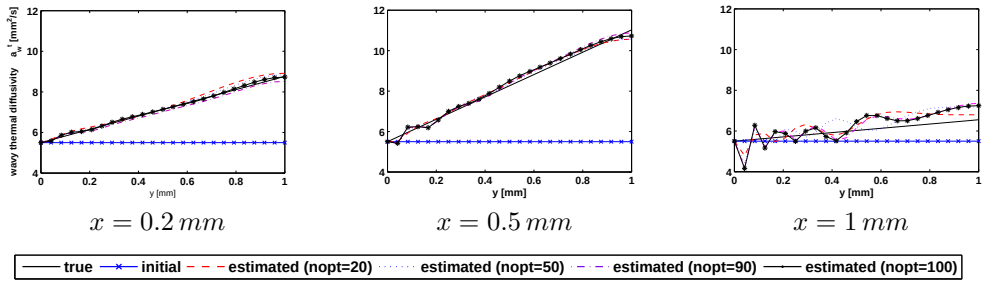

FIG. 5. *Estimated wavy thermal diffusivity a_w^t at different Newton iterations nopt, time $t = 0.01s$, different x and constant $z = 0.5\,mm$.*

the outflow boundary Γ_{out} the estimation quality of the source F_w in the previous step is impaired by the lack of information. At the outflow boundary, due to convection, there is not enough information to reconstruct the unknown founction from the available data.

The estimates of the wavy thermal diffusivity at different numbers of Newton iterations *nopt* as a functions of x for $y \in \{0.2, 0.5, 1\}\,mm$ and $z = 0.5\,mm$ at time $t = 0.01s$ are presented in Fig. 6, whereas Fig. 7 shows the estimation results at different numbers of Newton iterations for two later times $t \in \{0.03, 0.4\}s$. Because of the very good initial approximation, at large times (e.g. for $t = 0.4s$ in the figure) the convergence is achieved even before reaching $nopt = 5$.

In the third identification step the model parameters $\theta \in \mathbb{R}^5$ are estimated using the reconstructed transport coefficients $a_w^t(\mathbf{x})$ at times $t \in [0.01s, 0.5s]$ and the proposed model $f_{\mathrm{w}}(\mathbf{x}, t, \theta)$ (cf. (4.3)). Fig. 8 (a) shows the deviations between the reconstructed wavy thermal diffusivities $a_w^t(\mathbf{x})$ and the optimal solution $f_{\mathrm{w}}(\mathbf{x}, t, \theta^\star)$ for selected times $t \in \{0.01, 0.03, 0.4\}s$. A high reconstruction quality is achieved. The resulting optimal value for the model parameter vector

$$\theta^\star = (1.12, 1.05, 3.12, 0.02, 0.06)\,, \tag{4.6}$$

is in a good agreement with the exact value θ^{ex} in (4.4). In Fig. 8 (b) the estimation results for constant $y = 0.5\,mm$ and $z = 0.5\,mm$ at different identification steps of an incremental approach are presented together with the "true" wavy thermal diffusivity $a_w^t(\mathbf{x})$ (cf. (4.2b)) and their initial guesses for a detailed comparison. There

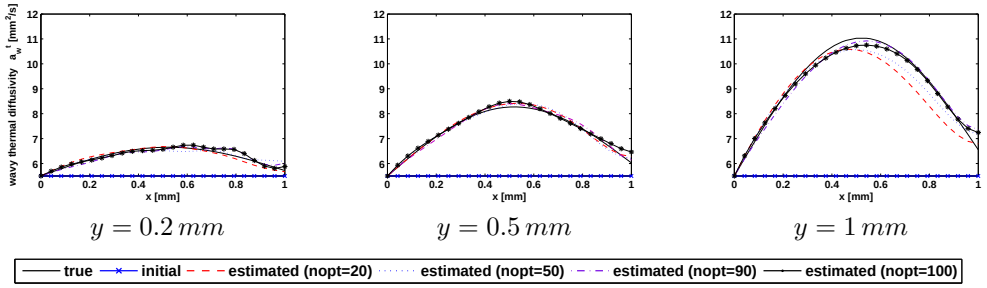

FIG. 6. *Estimated wavy thermal diffusivity a_w^t at different Newton iterations nopt, time $t = 0.01s$, different y and constant $z = 0.5\,mm$.*

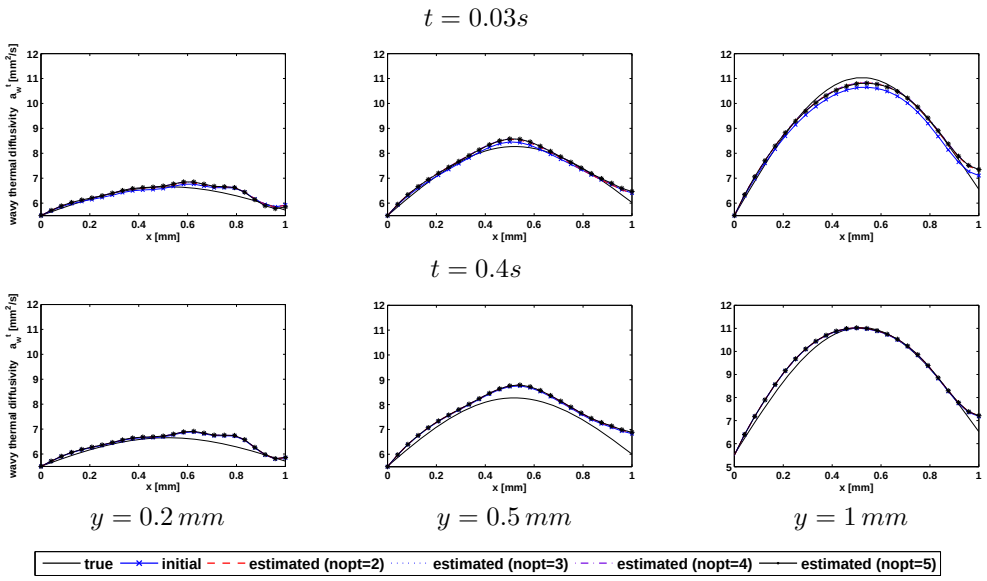

FIG. 7. *Estimated wavy thermal diffusivity a_w^t at different outer optimization iterations nopt, two different times, three different y and constant $z = 0.5\,mm$.*

is an obvious bias which can be atributed to error propagation in the incremental identification procedure [5]. This bias can be easily eliminated by a final simultaneous step which converges quickly due to very good initial values [9].

4.2. Estimation in the presence of measurement errors. In this section, we perturb the measured temperature T_m by an artificial measurement error ω. The values of ω are generated from a zero mean normal distribution with variance one. We compute the perturbed temperature $\tilde{T}_m$ by

$$\tilde{T}_m = T_m + \sigma\omega\,,$$

with σ being the standard deviation of the measurement error. The parameter σ is used to control the amount of error added to the exact data. We take the value $\sigma = 0.1$ in the following simulation experiments.

In the presence of measurement errors, an increasing number of iterations eventually leads to a poorer estimation quality due to the undesirable effect that measurement errors are resolved. Therefore, a compromise between the residual and the solution norm has to be established by an appropriate regularization [20]. Besides the (fixed) regularizing effect of time and space discretization, the number of optimization iterations is used as a regularization parameter. An appropriate value for this parameter can be obtained by the L-curve, which is a parameterized plot of the residual against a smoothing norm of the solution.

The results of source term estimation will be presented first. The L-curve plot is shown in Fig. 9. This curve suggests that $nopt = 100$ is a reasonable choice of the regularization parameter for the given value of σ. The snapshots of the regularized optimal estimates $F_w^{nopt}(\mathbf{x}, t)$ are shown in Fig. 10, for constant $z = 0.5\,mm$. Due to the errors in the measurements, the estimates are no longer smooth, but the qualitative behaviour is the same as for the case without measurement noise (cf. Fig. 3).

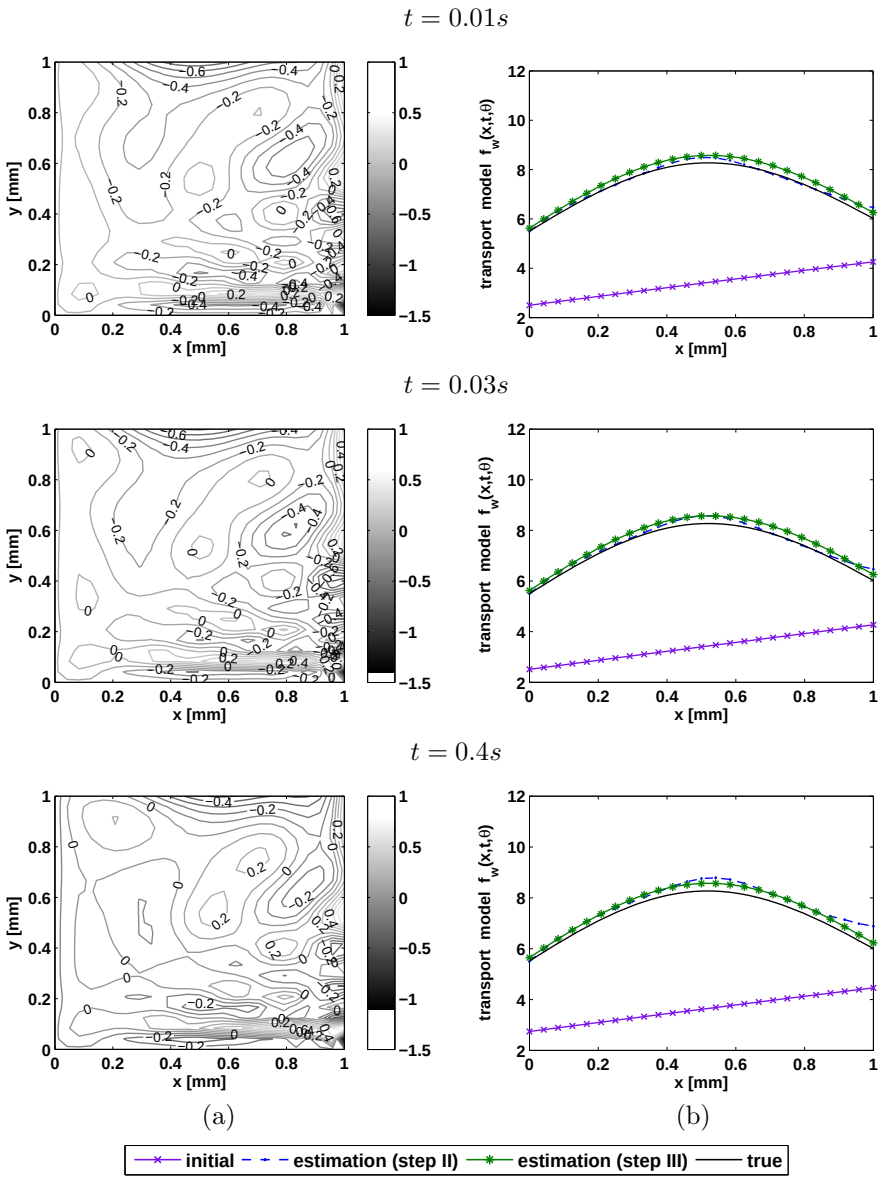

FIG. 8. *(a) Deviation between the wavy thermal diffusivity estimated in the second step and the model f_w estimated in the third step of the incremental approach (b) "true" wavy thermal diffusivity, estimated wavy thermal diffusivity a_w^t in the second step and estimated model f_w in the third step of the incremental approach at different times for constant $y = 0.5\,mm$ and $z = 0.5\,mm$*

The estimation $F_w^{nopt}(\mathbf{x}, t)$ obtained with perturbed data is compared to the estimates $F_w^{200}(\mathbf{x}, t)$ obtained with exact data in the previous section. The results are shown in Fig. 11 as a function of x for fixed $y = 0.5\,mm\,, z = 0.5\,mm$ and three different t-values. The corresponding temperatures, presented in Fig. 12, are very close as expected.

The regularization parameter can be determined alternatively using the discrep-

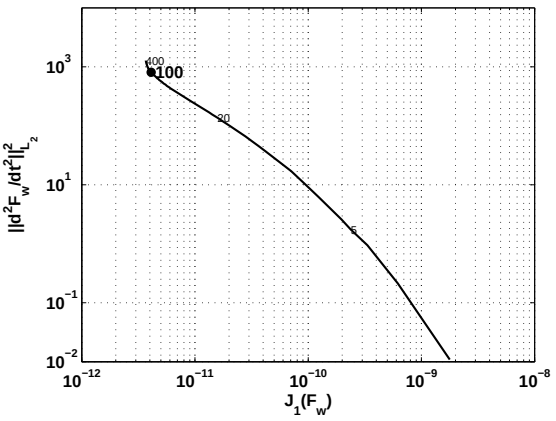

FIG. 9. *L-curve for source estimation based on perturbed measurements with* $\sigma = 0.1$.

ancy principle [14]. Here the knowledge of the error's magnitude is used to propose the stopping condition for the objective functional: the iterationsis stopped when the residual approximately equals the error level σ. Using (3.1), we get the condition

$$J_1(F_w^n) < \kappa_1 (t_f - t_0) V \sigma \,, \tag{4.7}$$

where V is the volume of Ω and $\kappa_1 > 1$. For a value of $\kappa_1 = 1.01$ the optimal number of iterations is $nopt = 16$ for a given error $\sigma = 0.1$. The estimate obtained at this point is smoother, however over-regularized, whereas the one suggested by the L-curve method shows oscillations but is closer to the estimations obtained with unperturbed data. Therefore, we took the estimates obtained by the L-curve principle in the next identification step.

For the estimation of the wavy thermal diffusivities $a_w^t(\mathbf{x})$ at times $t \in [0.01s, 0.5s]$, the regularized optimal solution $F_w^{nopt\,t}(\mathbf{x})$ and the measurement data $\tilde{T}_m^t$ are used in the corresponding direct problem (2.11) for a given time t. We apply the L-curve and the discrepancy principle in order to find the optimal value for the number of Newton iterations in the truncated Newton-CGNE method. We set the values $\eta = 0.98$ and $n_\star = 20$ in the stopping rule (3.14) for the inner iteration for all times $t \in [0.01s, 0.5s]$. The stopping condition for the Newton iteration based on the discrepancy principle is

$$J_2(a_w^{t\,k}) < \kappa_2 V \sigma \,. \tag{4.8}$$

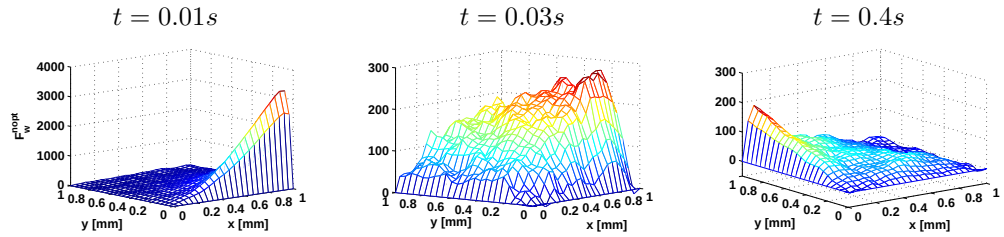

FIG. 10. *Estimated source* F_w *at different times for constant* $z = 0.5\,mm$ *with perturbed measurements* ($\sigma = 0.1$) *for* $nopt = 100$.

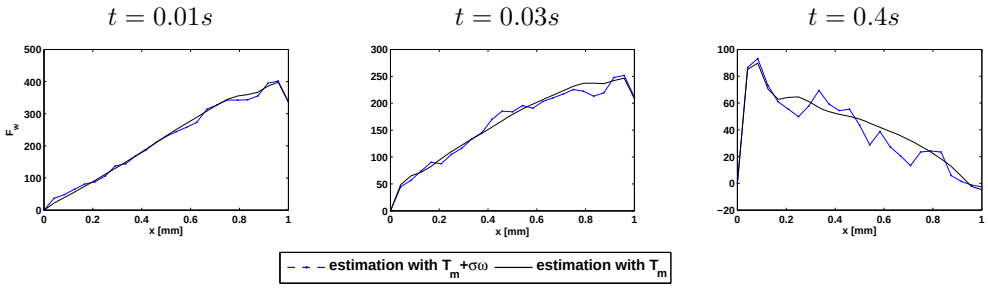

FIG. 11. *Estimated source F_w with unperturbed measurements for nopt = 200 and perturbed measurements for $\sigma = 0.1$ for (nopt = 100) at different times.*

In experiments we tried different values of $\kappa_2 > 1$ and always observed that the estimates obtained by the discrepancy principle are smoother but still over-regularized, whereas those suggested by the L-curve method contain oscillations but are closer to the exact quantity. The same result has been observed for source estimation in the first step for the example considered. A good understanding of the regularizing effects of the CG method is well developed for linear problems [20], whereas a practical understanding of the regularizing effect for the truncated Newton-CGNE method is rather speculative [18]. Nevertheless, the choice of an appropriate value for the regularization parameter is rather problem-dependent and relies to a large extent on user experience. In Fig. 13, the optimal regularized estimates for the chosen noise level $\sigma = 0.1$ obtained from the L-curve method are presented as a function of x for $z = 0.5\,mm$ and different values of y at selected times. Due to the reasons stated above in the noise-free case, we see again, that estimation quality decreases near the outflow at $x = 1\,mm$. Here, in contrast to the noise-free case, the estimates computed for $t = 0.01$ have been used as initial approximations for each later time $t > 0.01s$.

Finally, in order to estimate the model parameters $\theta \in \mathbb{R}^5$ in the model $f_{\mathrm{w}}(\mathbf{x}, t, \theta)$ (cf. (4.3)) the regularized optimal solutions $a_w^{t\ nopt}(\mathbf{x})$ at times $t \in [0.01s, 0.5s]$ are used. In Fig. 14 (a) the deviations between the optimal regularized wavy thermal diffusivity from the second step and the optimal, estimated model $f_{\mathrm{w}}(\mathbf{x}, t, \theta^\star)$ in the third step are presented for selected times. The resulted optimal value of the parameter

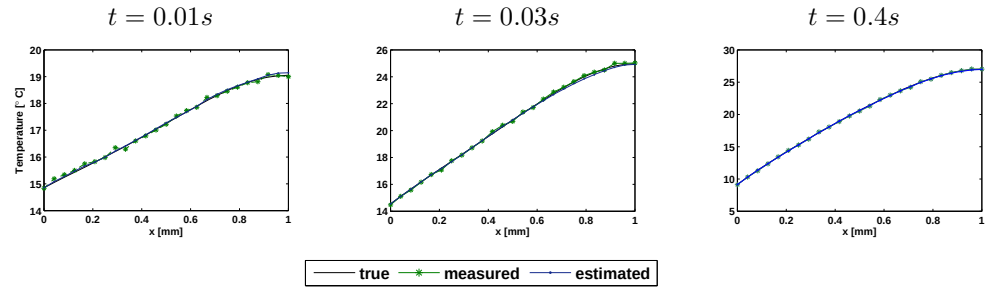

FIG. 12. *Exact, measured and estimated temperature for $\sigma = 0.1$ at different times.*

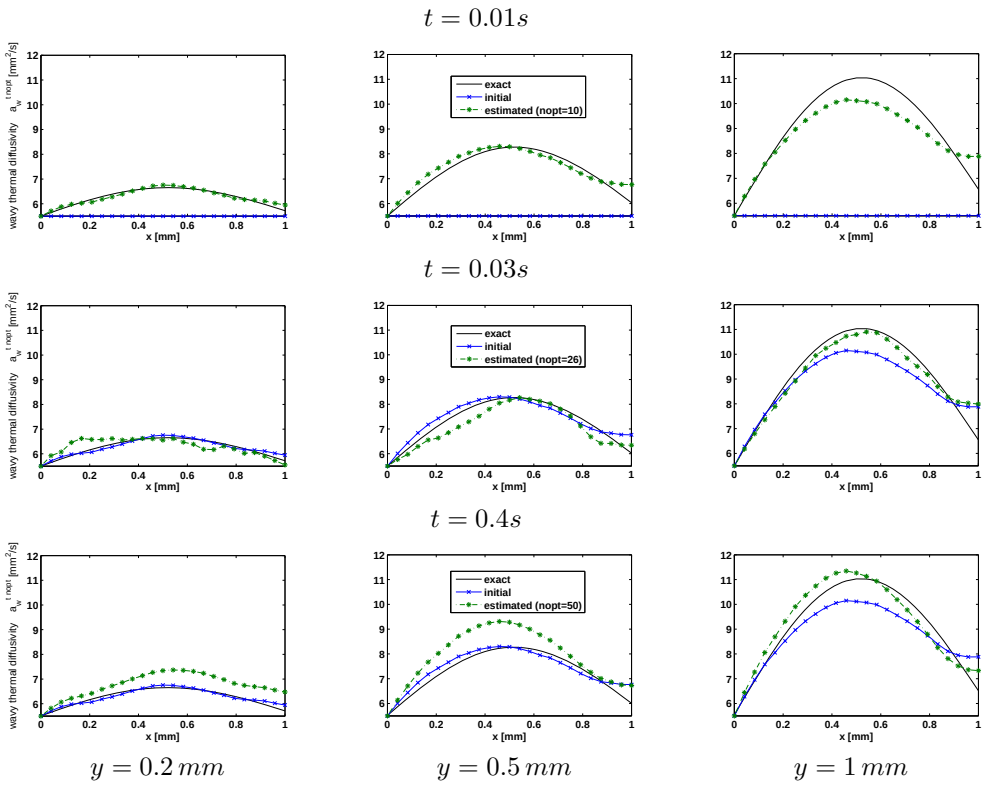

FIG. 13. *Estimated wavy thermal diffusivity* a_w^t *for noise level of* $\sigma = 0.1$ *after corresponding optimal nopt iterations at different times for constant* $z = 0.5\,mm$ *and different* y.

vector amounts to

$$\theta^\star = (1.15, 1.08, 3.17, 0.09, 0.08)\,. \tag{4.9}$$

In Fig. 14 (b) the estimations at different identification steps are presented once more together with the "true" wavy thermal diffusivity $a_w^t(\mathbf{x})$ (cf. (4.2a)) for constant $y = 0.5\,mm$ and $z = 0.5\,mm$ and selected times. The estimation quality has decreased compared to the noise-free case above, however, a quite good reconstruction has been achieved.

5. Conclusions. A novel method for the incremental identification of transport models for transport coefficients in convection-diffusion systems is presented. The simultaneous model is split into three hierarchically structured submodels. The identification problems in the first two steps (levels) have to be solved only once. The model for the transport coefficient has to be estimated in the third step.

The approach is illustrated for the identification of a model for an effective thermal diffusivity in a three dimensional convection-diffusion problem which is similar to a flat film model used to investigate energy transport in laminar wavy film flows. The first step of the incremental identification is rather easy to handle due to the linearity of the corresponding source inverse problem. The results obtained with a CG method at this level are quite satisfactory both for error-free and noisy measurements. The second step of the identification is far more complex due to the strong nonlinearity and

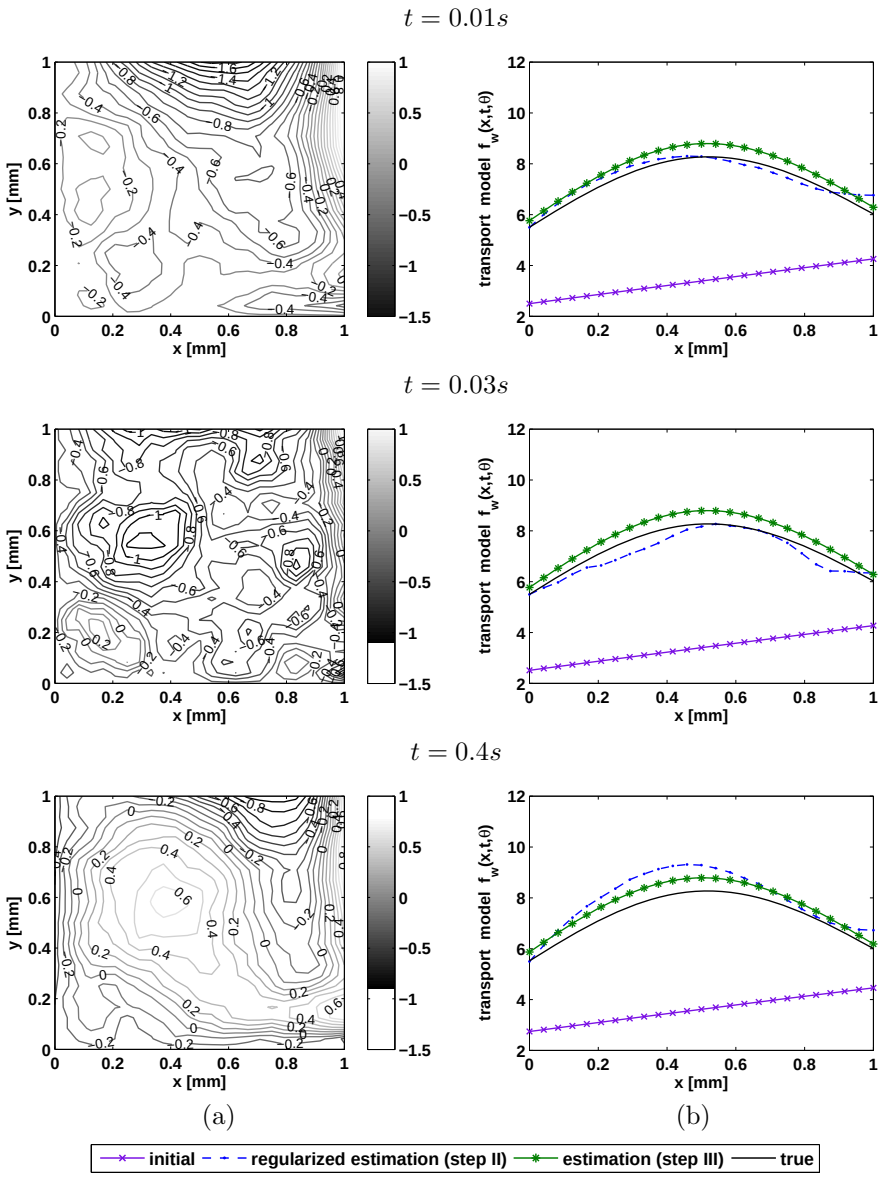

FIG. 14. *(a) Deviation between the regularized wavy thermal diffusivity estimated in the second step and the model f_w estimated in the third step of the incremental approach at different times for the noise-level $\sigma = 0.1$. (b) "true" wavy thermal diffusivity, regularized wavy thermal diffusivity a_w^{nopt} in the second step and estimated model f_w in the third step of the incremental approach at different times for constant $y = 0.5\,mm$ and $z = 0.5\,mm$ for the noise-level $\sigma = 0.1$.*

high degree of ill-posedness of the coefficient inverse problem that has to be solved. The truncated Newton-CGNE method, belonging to the class of inexact Newton-type methods, is used to solve this problem as it is known to be very suitable for such nonlinear inverse problems [14]. For good results one needs, however, an initial approximation which is sufficiently close to the solution. Finally, in the third step, a single model for the effective thermal diffusivity is considered and the parameter

estimation for it is carried out. The interplay between the tree steps both with and without measurement errors is investigated by means of an illustrative case study.

We have, for the first time, successfully applied the concept of incremental model identification to a complicated transport problem in 3D. This proof of concept should not address the model discrimination issue in the third step of the incremental approach, where the best model is chosen from a set of candidate models by discriminating between the candidates using some reasonable model fit criterion [31].

Future work will address the following issues in addition to model discrimination. Robust regularization techniques will be studied in more detail. Besides the number of iterations, the discretization in space and time has a regularizing effect which needs to be properly exploited in an appropriate discretization framework. Furthermore, ill-posedness can be handled by adding a (Tikhonov) regularization term to the corresponding objective functional, cf. [14]. The interplay between such a regularization on the level of the problem with those regularizing effects in the numerical method, have to be analysed carefully (see e.g. [4, 7]). A further issue is a better theoretical understanding of the error propagation through the sequence of inverse problems in the incremental approach similar to [5]. Finally, in this paper we do not present a detailed comparison with the simultaneous approach (as in [5]), which is also a topic of current research.

Acknowledgements. The authors gratefully acknowledge the financial support of Deutsche Forschungsgemeinschaft (DFG) within the Collaborative Research Center (SFB) 540 "Model-based experimental analysis of kinetic phenomena in fluid multiphase reactive systems".

REFERENCES

[1] O. M. Alifanov, *Inverse Heat Transfer Problems*, Springer, Berlin, 1994.

[2] O. M. Alifanov, E.A. Artyukhin, and S.V. Rumyantsev, *Extreme Methods for Solving Ill-Posed Problems with Applications to Inverse Heat Transfer Problems*, Begell House, Inc., U.S.A., 1995.

[3] O. M. Alifanov, Y. Jarny, P.V. Prosuntsov, and G.A. Ivanov, *Complex identification of thermophysical properties of anisotropic composite material*, in Proceedings of the 5th international Conference on Inverse Problems in Engineering: Theory and Practice, Cambridge, U.K., 2005.

[4] U. Ascher and E. Haber, *A multigrid method for distributed parameter estimation problems*, Electronic Transactions on Numerical Analysis, 15 (2003), pp. 1–17.

[5] A. Bardow and W. Marquardt, *Incremental and simultaneous identification of reaction kinetics: methods and comparison*, Chem. Eng. Sci., 59 (2003), pp. 2673–2684.

[6] ———, *Identification of diffusive transport by means of an incremental approach*, Comp. Chem. Eng., 28 (2004), pp. 585–595.

[7] Th. Binder, L. Blank, W. Dahmen, and W. Marquardt, *On the regularization of dynamic data reconciliation problems*, 12 (2002), pp. 557–567.

[8] H. Brauer, *Strömung und Wärmeübergang bei Rieselfilmen*, in VDI-Forsch.-Heft 457, VDI-Verlag, Düsseldorf, 1956.

[9] M. Brendel, D. Bonvin, and W. Marquardt, *Incremental identification of kinetic models for homogeneous reaction systems*, Chem. Eng. Sci., 61 (2006), pp. 5404–5420.

[10] R. S. Brodkey and H. C. Hershey, *Transport Phenomena — A Unified Approach*, McGraw-Hill Book Company, U.S.A, 1976.

[11] M. J. Colaco, G. S. Dulikravich, H. R. B. Orlande, and F. A. Rodrigues, *A comparison of two solution techniques for the inverse problem of simultaneously estimating the spatial variations of diffusion coefficient and source terms*, in Proceedings of IMECE'03, 2003 ASME International Mechanical Engineering Congress and Exposition, Washington, D.C., U.S.A., 2003.

[12] G. Dietze, V.V. Lel, and R. Kneer, *Modelling of heat transfer in stable wavy film flow based on effective thermal diffusivity*, in Proceedings of IHTC-13 2006, Sidney, 2006.

[13] *DROPS package*. http://www.igpm.rwth-aachen.de/DROPS/.
[14] H. W. Engl, M. Hanke, and A. Neubauer, *Regularization of Inverse Problems*, Kluwer Academic Publishers, Dordrecht, 1996.
[15] R. Fletcher and C. M. Reeves, *Function minimization by conjugate gradients*, J. Comput., 7 (1964), pp. 149–154.
[16] A. L. Frenkel and K. Indireshkumar, *Wavy film flows down an inclined plane: Perturbation theory and general evolution equation for the film thickness*, Phys. Rev. E, 60 (1999), pp. 4143–4157.
[17] S. Gross, M. Soemers, A. Mhamdi, F. Al Sibai, A. Reusken, W. Marquardt, and U. Renz, *Identification of boundary heat fluxes in a falling film experiment using high resolution temperature measurements*, Int. J. Heat Mass Tran., 48 (2005), pp. 5549–5562.
[18] M. Hanke, *Regularizing properties of a truncated Newton-CG algorithm for nonlinear inverse problems*, Numer. Funct. Anal. Optim., 18 (1998), pp. 971–993.
[19] M. Hanke and O. Scherzer, *Error analysis of an equation error method for the identification of the diffusion coefficient in a quasi-linear parabolic differential equation*, SIAM J. Appl. Math., 59 (1999), pp. 1012–1027.
[20] C. Hansen, *Rank-Deficient and Discrete Ill-posed Problems: Numerical Aspects of Linear Inversion*, SIAM Monographs on Mathematical Modeling and Computation, SIAM, Philadelphia, 1998.
[21] T. Hastie, R. Tibshirani, and J. Friedman, *The elements of statistical learning: Data mining, Inference, and Prediction*, Springer Verlag, New York, 2001.
[22] J. P. Kaipio and E. Somersalo, *Computational and Statistical Methods for Inverse Problems*, Springer Verlag, New York, 2004.
[23] W. Marquardt, *Towards a process modeling methodology*, vol. 293 of NATO-ASI Series, Kluwer Academic Pub., Dordrecht, 1995, pp. 3–41.
[24] ———, *Model-based experimental analysis of kinetic phenomena in multi-phase reactive systems*, Chem. Eng. Res. Des., 83 (2005), pp. 561–573.
[25] J. Nocedal and S. J. Wright, *Numerical Optimization*, Springer Series in Operations Research, Springer, Berlin, Heidelberg, New York, 1999.
[26] M.K. Panga, R. R. Mudunuri, and V. Balakotaiah, *Long-wavelength equation for vertically falling films*, Phys. Rev. E, 71 (2005), p. 036310.
[27] L. Prandtl, *Über Flüssigkeitsbewegung bei sehr kleiner Reibung*, in Gesammelte Abhandlungen zur angewandten Mechanik, Hydro- und Aerodynamik, W. Tolmien, H. Schlichting, and H. Görtler, eds., vol. 2, Springer-Verlag, Berlin, 1961.
[28] G.R. Richter, *Numerical identification of a spatially varying diffusion coefficient*, Math. Comput., 36 (1981), pp. 375–386.
[29] Y. Saad, *Iterative Methods for Sparse Linear Systems*, SIAM, Philadelphia, PA, USA, 2003.
[30] J. Su and F. H. Geoffrey, *Inverse heat conduction problem of estimating time-varying heat transfer coefficient*, Numer. Heat Transf., 45 (2004), pp. 777–789.
[31] E. Walter and L. Pronzato, *Identification of Parametric Models from Experimental Data*, Springer, Berlin, 1997.
[32] W. Wilke, *Wärmeübergang an Rieselfilmen*, in VDI-Forsch.-Heft 490, VDI-Verlag, Düsseldorf, 1962.